DOI 10.1007/s11029-021-09959-w
Mechanics of Composite Materials, Vol. 57, No. 3, July, 2021 (Russian Original Vol. 57, No. 3, May-June, 2021)

COMBINED USE OF CONTACT LAYER AND FINITE-ELEMENT METHODS TO PREDICT THE LONG-TERM STRENGTH OF ADHESIVE JOINTS IN NORMAL SEPARATION

A. S. Chepurnenko, S. V. Litvinov,* and S. B. Yazyev

Keywords: *creep, adhesive joints, contact layer method, finite-element method, long-term strength.*

A new approach to the analysis of the stress-strain state of adhesive joints and the transverse strength of layered composites is proposed. It consists in a combined use of finite-element and contact layer methods. Based on this approach, the problem of the long-term strength in normal separation of two adhesively bonded disks glued together by an epoxy resin, which was previously considered by R. A. Turusov, is solved. The nonlinear Maxwell–Gurevich equation is used as the law of adhesion creep. The model constructed by R. A. Turusov does not take into account the shear creep strains of contact layer and is based on the hypothesis of linear distribution of shear stresses across the thickness of adhesive layer and substrate. It was found that these simplifications lead to overestimated tangential stresses. By analyzing the creep law with time tending to infinity, the long-term elastic modulus and Poisson ratio of the adhesive are derived and the reliability of their values is confirmed.

Introduction

To analyze the stress-strain state of adhesive joints and the transverse strength of laminated composites, the contact layer method is often used. A large number of solutions based on this method belongs to R. A. Turusov [1-14]. The method based on the assumption that, between the adhesive and substrate, there is an intermediate layer with properties different from those of the contacting pair. The concept of contact layer is described in more detail in [9, 13-15]. The contact layer in [1-14] is presented in the form of a brush of short vertical elastic bonds operating only in tension, compression, and

Faculty of Industrial and Civil Engineering, Don State Technical University, Rostov-on-Don, 344022 Russian Federation
*Corresponding author; e-mail: litvstep@gmail.com, anton_chepurnenk@mail.ru

Translated from Mekhanika Kompozitnykh Materialov, Vol. 57, No. 3, pp. 517-534, May-June, 2021. Original article submitted April 15, 2020; revision submitted February 25, 2021.

shear. This approach makes it possible to obtain a solution based on the existing apparatus of elasticity and creep theories. The contact layer method allows one to solve problems on determining the concentration of shear stresses arising at layer boundaries and corner points, where the solution based on the classical elasticity theory leads to infinite stresses.

In all the publications mentioned, the solution is carried out by direct integration of differential equations, either analytically or numerically. In this case, to obtain the resolving equations, additional simplifications are introduced; in particular, the hypothesis of a linear distribution of shear stresses across the thickness of adhesive and substrate. In this paper, it is shown that the contact-layer method in combination with the finite-element method (FEM), can be used for this purpose, which makes it possible to avoid this simplification and to obtain a more accurate solution. Also, in distinction to works [1-14], the contact layer here is endowed with rheological properties.

In essence, close to the approach proposed by the authors is the AEM (Applied Element Method) method, where the body is represented as a set of absolutely rigid elements connected by normal and shear springs, responsible for the transfer of normal and tangential stresses, respectively, between the elements [16, 17]. Material parameters in the AEM are set by assigning an appropriate stiffness to the springs. The distinction from the approach proposed is the fact that the elements and springs have a finite stiffness. The AEM method has become widespread mainly in problems of structural calculations for the progressive collapse [18-20] and has not been used in the mechanics of polymers and composite materials, with the exception of work [17].

We will consider the problem of creep of adhesive joints in two statements. In the first one, the nonlinearity of distribution of shear stresses across the thickness of layers is neglected, and the solution is performed by the finite-difference method. In the second formulation, this nonlinearity is taken into account, and the solution is performed by the finite-element method. However, the rheological properties of contact layer are considered in both the statements.

1. Solution disregarding the nonlinearity of distribution of shear stresses across the thickness of adhesive and substrate

Let us consider an adhesion joint of two discs subjected to the normal separation. The calculation diagram is shown in Fig. 1. This problem was first solved in [9]; however, as already noted, this solution contains some simplifications and inaccuracies.

The system of initial equations in [9] is written as

$$\frac{\partial \sigma_{r0}}{\partial r} + \frac{\sigma_{r0} - \sigma_{\varphi 0}}{r} + \frac{\tau}{h_0} = 0\,,$$

$$\frac{\partial \sigma_{r1}}{\partial r} + \frac{\sigma_{r1} - \sigma_{\varphi 1}}{r} - \frac{\tau}{\bar{h}_1} = 0\,,$$

$$\frac{\partial}{\partial r}(\sigma_{\varphi 0} - \mu_0 \sigma_{r0}) = \frac{1+\mu_0}{r}(\sigma_{r0} - \sigma_{\varphi 0})$$

$$\times \frac{\partial}{\partial r}(\sigma_{\varphi 1} - \mu_1 \sigma_{r1}) = \frac{1+\mu_1}{r}(\sigma_{r1} - \sigma_{\varphi 1}) + E_1 \left(\frac{\varepsilon^*_{r1} - \varepsilon^*_{\varphi 1}}{r} - \frac{\partial \varepsilon^*_{\varphi 1}}{\partial r} \right)\,, \tag{1}$$

$$\frac{h^*}{G}\frac{\tau}{r} = \frac{\sigma_{\varphi 1} - \mu_1 \sigma_{r1}}{E_1} - \frac{\sigma_{\varphi 0} - \mu_0 \sigma_{r0}}{E_0}$$

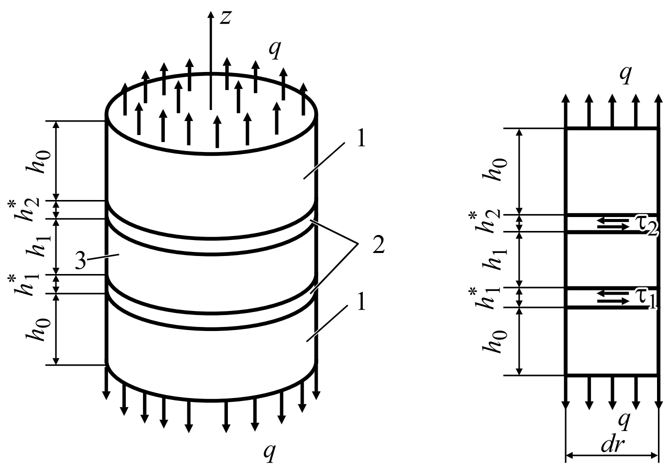

Fig. 1. Calculation diagram of an adhesive joint: 1 — substrate, 2 — boundary layers, and 3 — adhesive.

$$-q\left(\frac{\mu_1}{E_1}-\frac{\mu_0}{E_0}\right)+(\varepsilon_{t,1}-\varepsilon_{t,0})+(\varepsilon_{c,1}-\varepsilon_{c,0})+\varepsilon_{\varphi 1}^*.$$

Here, the subscript 0 points to the substrate, 1 — to the adhesive; $\overline{h}_1 = h_1/2$, $h^* = h_1^* = h_2^*$, and $\tau = \tau_1 = -\tau_2$ are shear stresses in contact layers.

Let us compare formulas (1) with basic relations of the mechanics of deformable solids, which, for axisymmetric problems, are written as

a) equilibrium equation

$$\frac{\partial \sigma_r}{\partial r}+\frac{\sigma_r-\sigma_\varphi}{r}+\frac{\partial \tau_{rz}}{\partial z}=0, \tag{2}$$

b) compatibility equation

$$\frac{\partial \varepsilon_\varphi}{\partial r}+\frac{\varepsilon_\varphi-\varepsilon_r}{r}=0, \tag{3}$$

c) and physical equations

$$\begin{aligned} \varepsilon_r &= \frac{1}{E}\left[\sigma_r-\mu(\sigma_\varphi+\sigma_z)\right]+\varepsilon_t+\varepsilon_c+\varepsilon_r^*, \\ \varepsilon_\varphi &= \frac{1}{E}\left[\sigma_\varphi-\mu(\sigma_r+\sigma_z)\right]+\varepsilon_t+\varepsilon_c+\varepsilon_\varphi^*, \end{aligned} \tag{4}$$

where ε_t is the thermal strain, ε_c is the chemical shrinkage strain, and ε_r^* and ε_φ^* are creep strains.

The substrate is assumed elastic, i.e., its creep strains are not taken into account.

An analysis of the first two equations in (1) shows that they have been obtained on the basis of Eq. (2) on the assumption that shear stresses across the thickness of substrate and adhesive vary linearly (see Fig. 2). The third and fourth equations in (1) were obtained inserting (4) into (3) considering that $\sigma_z = q = \text{const}$. Let us dwell separately on the fifth equation in (1). We rewrite it as

$$\tau = G\frac{1}{h^*}r\left[\frac{\sigma_{\varphi 1}-\mu_1\sigma_{r1}}{E_1}-\frac{\sigma_{\varphi 0}-\mu_0\sigma_{r0}}{E_0}\right.$$

$$\left.-q\left(\frac{\mu_1}{E_1}-\frac{\mu_0}{E_0}\right)+(\varepsilon_{t,1}-\varepsilon_{t,0})+(\varepsilon_{c,1}-\varepsilon_{c,0})+\varepsilon_{\varphi 1}^*\right]. \tag{5}$$

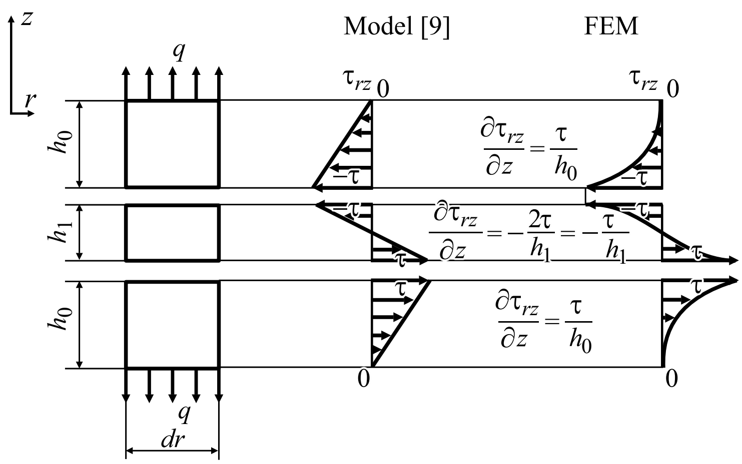

Fig. 2. Distribution of shear stresses across the thickness of adhesive and substrate in model [9] and by the FEM.

The expression in the square brackets is the difference between the circumferential strains of contact layer and substrate, $\Delta\varepsilon_\varphi$. Since the radial displacements u are related to circumferential strains as $\varepsilon_\varphi = u / r$, the product $\Delta\varepsilon_\varphi \cdot r$ is the difference between the radial displacements Δu of substrate and contact layer. The ratio $\Delta u / h^*$ is the shear angle of the contact layer, i.e., Eq. (5) can be rewritten as

$$\tau = G\gamma_{rz} .$$

However, such a relationship between shear stresses and shear strains is valid only for an elastic material. Let us assume that the contact layer is viscoelastic, i.e., the total strain is the sum of elastic and creep strains,

$$\gamma_{rz} = \frac{\tau}{G} + \gamma_{rz}^* . \tag{6}$$

The hypothesis that the contact layer is viscoelastic was introduced in order to take into account the shear creep, since the final resolving equation in [9] does not contain shear creep strains of layers, although, in this problem, shear stresses are present in all layers and determine the strength of the adhesive joint.

Expressing from (6) the tangential stresses in terms of strains, we obtain

$$\tau = G(\gamma_{rz} - \gamma_{rz}^*) = G\left\{ \frac{r}{h^*}\left[\frac{\sigma_{\varphi 1} - \mu_1\sigma_{r1}}{E_1} - \frac{\sigma_{\varphi 0} - \mu_0\sigma_{r0}}{E_0} \right.\right.$$

$$\left.\left. -q\left(\frac{\mu_1}{E_1} - \frac{\mu_0}{E_0} \right) + (\varepsilon_{t,1} - \varepsilon_{t,0}) + (\varepsilon_{c,1} - \varepsilon_{c,0}) + \varepsilon_{\varphi 1}^* \right] - \gamma_{rz}^* \right\} . \tag{7}$$

The final resolving equation for the shear stress in the contact layer, derived from the first four equations in (1) and Eq. (7), takes the form

$$\frac{\partial^2\tau}{\partial r^2} + \frac{1}{r}\frac{\partial\tau}{\partial r} - \tau\left(\frac{1}{r^2} + c^2 \right) = \frac{G}{h^*}\frac{1}{r^2}\frac{\partial}{\partial r}\left[r^2(\varepsilon_{r1}^* - \varepsilon_{\varphi 1}^*) \right]$$

$$-\frac{G}{h^*}\frac{\xi(r,t)(1+\mu_1)}{E_1}-G\left(\frac{\partial^2\gamma_{rz}^*}{\partial r^2}+\frac{1}{r}\frac{\partial\gamma_{rz}^*}{\partial r}-\frac{\gamma_{rz}^*}{r^2}\right), \tag{8}$$

where $A^2=\frac{G}{h^*}\left(\frac{1-\mu_1^2}{E_1\overline{h}_1}-\frac{1-\mu_0^2}{E_0h_0}\right)$ and $\xi(r,t)=E_1\left(\frac{\varepsilon_{r1}^*-\varepsilon_{\varphi 1}^*}{r}-\frac{\partial\varepsilon_{\varphi 1}^*}{\partial r}\right)$.

In [9], the last two terms are absent from the right-hand side of the final resolving equation. The author of work [9] apparently neglected the first of the indicated terms, and the second term appears owing to the shear creep, which was not taken into account in [9].

Let us consider further boundary conditions. It follows from symmetry of the problem that $\tau=0$ at $r=0$. For normal stresses, we take boundary conditions in the form

$$r=0:\sigma_{r0}=\sigma_{\varphi 0},\sigma_{r1}=\sigma_{\varphi 1};\quad r=R:\sigma_{r0}=0,\sigma_{r1}=0. \tag{9}$$

Based on (9) and the first four equations in (1) and (7), the boundary condition for the tangential stresses at $r=R$ can be written as

$$m\frac{\partial\tau}{\partial r}+(1-m)\frac{\tau}{R}=\frac{G}{h^*}\Big[Q(R,t)-f(R,t)$$

$$+mR\left(\frac{\xi(R,t)}{E_1}+\frac{\partial Q}{\partial r}\right)+m(1+\mu_0)f(R,t)\Big], \tag{10}$$

where $m=\frac{G}{h^*c^2}\left(\frac{1-\mu_1}{\overline{h}_1E_1}+\frac{1-\mu_0}{h_0E_0}\right)$, $Q(r,t)=-q\left(\frac{\mu_1}{E_1}-\frac{\mu_0}{E_0}\right)+(\varepsilon_{t,1}-\varepsilon_{t,0})+(\varepsilon_{c,1}-\varepsilon_{c,0})+\varepsilon_{\varphi 1}^*-\frac{h^*}{r}\gamma_{rz}^*$,

$$f(R,t)=\frac{(1-\mu_0)\overline{h}_1}{E_0(1-\mu_1)h_0}\frac{1}{R^2}\int_0^R\xi(r,t)r^2dr.$$

In [9], condition (10) has the same form, but there are no terms containing $f(R,t)$, and the shear creep strain γ_{rz}^* is absent from the expression for $Q(r,t)$.

2. Methodology of finite-element implementation of the problem

As already mentioned, using the finite-element method, it is possible to obtain a solution taking into account the nonlinear distribution of shear stresses across the thickness of adhesive and substrate. The adhesive and substrate are modeled by triangular axisymmetric finite elements, and the contact layer — by rods resisting only σ_z and τ_{rz} stresses. The finite-element model of the joint is shown in Fig. 3, where the finite-element mesh is shown schematically. Here we use a nonuniform division, with condensation at the corner point, at which the highest shear stresses arise; b_i^* is the width of the area represented by each bar.

When solving the problem by the finite-element method without using a contact layer, owing to the thickening of the mesh, the maximum stress increases indefinitely.

The strains of the finite element (FE) of the contact layer (Fig. 4) are determined as follows:

$$\gamma_{rz}=\frac{u_2-u_1}{h^*},\quad \varepsilon_z=\frac{w_2-w_1}{h^*}. \tag{11}$$

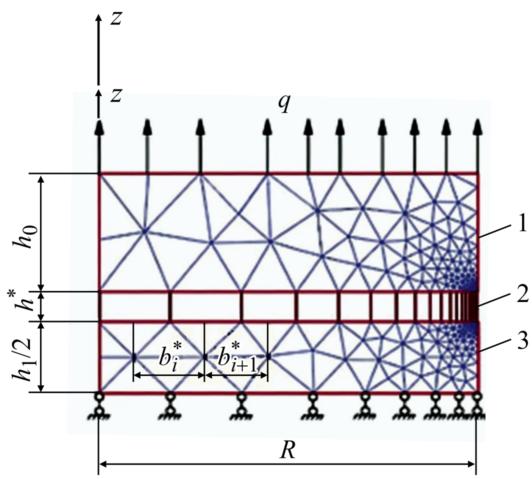

Fig. 3. Finite-element model of the adhesive joint: 1 — substrate, 2 — rods of the contact layer, and 3 — adhesive.

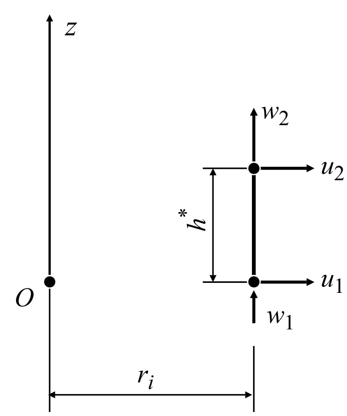

Fig. 4. Scheme of the finite element of the contact layer.

Relations (11) can be written in the matrix form

$$\{\varepsilon\} = \begin{Bmatrix} \varepsilon_z \\ \gamma_{rz} \end{Bmatrix} = \frac{1}{h^*} \begin{bmatrix} 0 & -1 & 0 & 1 \\ -1 & 0 & 1 & 0 \end{bmatrix} \{U\} = [B]\{U\},$$

where $\{U\} = \{u_1 \quad w_1 \quad u_2 \quad w_2\}^T$ is the vector of nodal displacements.

The relationship between stresses and strains in the contact layer, taking into account the creep, can be written as

$$\{\sigma\} = \begin{Bmatrix} \sigma_z \\ \tau_{rz} \end{Bmatrix} = \begin{bmatrix} E & \\ & G \end{bmatrix} \left(\begin{Bmatrix} \varepsilon_z \\ \gamma_{rz} \end{Bmatrix} - \begin{Bmatrix} \varepsilon_z^* \\ \gamma_{rz}^* \end{Bmatrix} \right)$$

$$= [D]\left(\{\varepsilon\} - \{\varepsilon^*\}\right) = [D]\{\varepsilon^{el}\},$$

where $\{\varepsilon^{el}\}$ is the vector of elastic strains, representing the difference between the total and creep strains.

The potential deformation energy of FE of the contact layer is described by the relation

$$W = \frac{1}{2}\int_V \{\sigma\}^T \{\varepsilon^{el}\} dV = 2\pi r_i b_i^* h^* \left[\frac{1}{2}\{U\}^T [B]^T [D][B]\{U\}\right.$$

$$\left. -\{U\}^T [B]^T [D]\{\varepsilon^*\} + \frac{1}{2}\{\varepsilon^*\}^T [D]\{\varepsilon^*\}\right]. \tag{12}$$

The width of the area represented by an i th rod is defined as

$$b_i^* = \frac{(r_{i+1} - r_{i-1})(r_{i-1} + r_i + r_{i+1})}{6r_i}. \tag{13}$$

Here, r_{i+1} and r_{i-1} are coordinates of the nodes at the junction of the contact layer with the adhesive (substrate) adjacent to the i th node. For $r = 0$ and $r = R$ ($i = 0$ and $i = n$), the products $r_i b_i^*$ are defined as

$$rb^*\Big|_0 = \frac{r_1^2}{6}, \quad r\,b^*\Big|_n = \frac{-r_{n-1}^2 - r_n r_{n-1} + 2r_n^2}{6}. \tag{14}$$

Initially, formulas (13) and (14) were obtained when the distributed load was reduced to nodes from the condition that its work is equal to the work of equivalent concentrated forces.

The stiffness matrix of FE of the contact layer based on (12) is defined as

$$[K_i] = 2\pi r_i b_i^* h^* [B]^T [D][B].$$

We will not consider here the construction of FEM equations for a triangular FE of the axisymmetric problem; this procedure is described in detail, for example, in [21]. Finally, after applying the principle of minimum total energy, the problem is reduced to the system of equations

$$[K]\{U\} = \{F\} + \{F^*\},$$

where $\{F\}$ is the vector of external nodal loads and $\{F^*\}$ is the contribution of creep strains to the load vector.

For the FE contact layer, the vector $\{F^*\}$ based on (12) is written as

$$\{F_i^*\} = 2\pi r_i b_i^* h^* [B]^T [D]\{\varepsilon^*\}.$$

The calculation was performed step by step, with the elastic problem solved at the first step. Using the calculated stresses, the growth rates of creep strains are determined, and then the creep strains at the next step were found by the Euler method.

3. Results and discussion

The calculation was carried out for an adhesive joint in which aluminum was the substrate and an EDT-10 epoxy resin the adhesive. The following initial data were used: R = 12 mm, $E_0 = 2 \cdot 10^5$ MPa, E_1 = 2867 MPa, h_0 = 1.2 mm, h_1 = 0.1 mm, $\mu_0 = 0.33$, $\mu_1 = 0.37$, and G / h^* = 9600 MPa/mm. The generalized nonlinear Maxwell–Gurevich equation was employed as the EDT-10 creep law, where creep strains are presented as the sum of spectrum components:

$$\varepsilon_{ij}^* = \sum_{s=1}^{n} (\varepsilon_{ij}^*)_s, \quad i = r, \varphi, z; \quad j = r, \varphi, z. \tag{15}$$

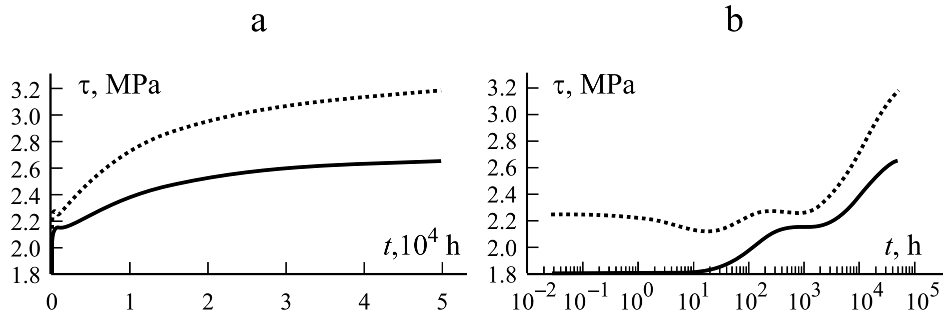

Fig. 5. The maximum tangential stress τ in the contact layer as a function of time t : $(\cdots)$ — FDM equation (8) and (——) — FEM (a); the same in the logarithmic scale (b).

When solving practical problems, as a rule, one or two members of the spectrum are limited [22-24]. The growth rate of creep strains was related to stresses by the equation

$$\frac{\partial(\varepsilon_{ij}^*)_s}{\partial t} = \frac{(f_{ij}^*)_s}{\eta_s^*}. \tag{16}$$

Here, $(f_{ij}^*)_s$ are stress functions; η_s^* is the relaxation viscosity, determined by the formulas

$$(f_{ij}^*)_s = \frac{3}{2}(\sigma_{ij} - p\delta_{ij}) - E_{\infty s}(\varepsilon_{ij}^*)_s,$$

$$\eta_s^* = \eta_{0s} \exp\left\{-(1/m_s^*)\left[\frac{3}{2}(\sigma_{pp} - p) - E_{\infty s}(\varepsilon_{pp}^*)_s\right]_{\max}\right\}, \tag{17}$$

where $p = \left(\sigma_r + \sigma_\varphi + \sigma_z\right)/3$ is the average stress; $E_{\infty s}$ is the modulus of high-elasticity; η_{0s} is the initial relaxation viscosity; m_s^* is the modulus of creep rate; δ_{ij} is the Kronecker symbol. The subscripts pp correspond to the principal stresses. Note that $\gamma_{rz}^* = 2\varepsilon_{rz}^*$. More details of the creep law can be found, for example, in [25].

In calculations, two members of the spectrum of relaxation times were taken into account with the following rheological parameters of EDT-10: $E_{\infty 1}$ = 2071 MPa, $E_{\infty 2} = 0.1E_{\infty 1}$, $m_1^* = m_2^*$ = 3.19 MPa, $\eta_{0.1} = 8.95 \cdot 10^9$ MPa·s, and $\eta_{0.2} = 8.72 \cdot 10^{10}$ MPa·s. The calculation by the FEM was performed using a program developed by the authors in the Matlab package. Equation (8) was solved by the finite-difference method (FDM) in combination with the Euler method.

In Fig. 5a, graphs of the time-dependent maximum tangential stresses in the contact layer (at $r = R$) are plotted at q = 10 MPa. In the first case, the obtained by the FDM were equal to 2.24 MPa at t = 0 and to 3.18 MPa at t = 50,000 h. When using the FEM, the stresses were 1.84 MPa at t = 0 and 2.65 MPa at t = 50,000 h. Qualitatively, according to both the methods, the stresses grew during the creep process, but this result is of limited nature. The horizontal section of the graph given by the FEM corresponds to the instant of time when the “senior” component ε_1^* of the spectrum of EDT-10 relaxation time decays. Then the “younger” component ε_2^* began to manifest itself. When using the model used in [10], at this moment in time, there arose a slight drop in stresses, which grew further. The same graph is shown in Fig. 5b in the logarithmic scale.

The deviation of the results is due to the fact that, in the model used in [9], a linear distribution of shear stresses across the thickness of the adhesive and substrate is assumed. When calculating by the FEM, it was found that the distribution of stresses across the substrate thickness was highly nonlinear. The shear stress in the substrate as a function of r and z at t = 0 is shown in Fig. 6. Due to the pronounced edge effect, only the area immediately adjacent to the point $r = R$ is shown. In the adhesive, the stress distribution across its thickness was close to linear.

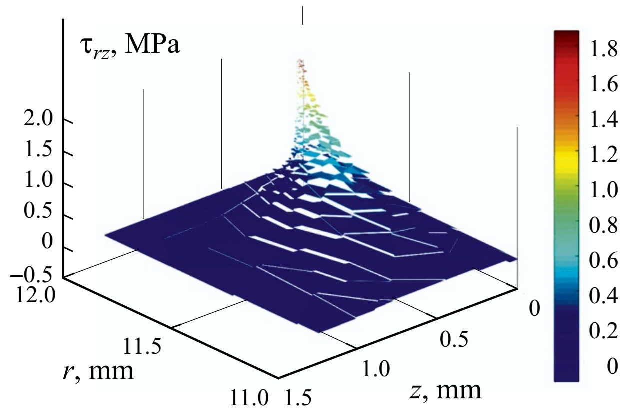

Fig. 6. The shear stress τ_{rz} in the substrate as a function of r and z at $t = 0$.

To control the correctness of the results, let us analyze Eqs. (15) - (17) at $t \to \infty$. If at the end of the creep process the stresses and deformations tend to a finite value, then, at $t \to \infty$, the growth rates of all creep strains and, hence, the corresponding stress functions, have to be equal to zero:

$$(f_{ij}^*)_s = 0 \to \frac{3}{2}(\sigma_{ij} - p\delta_{ij}) - E_{\infty s}(\varepsilon_{ij}^*)_s = 0. \tag{18}$$

From (18), one can find the creep strains at $t \to \infty$ by the formulas

$$\varepsilon_{r,s}^* = \frac{1}{E_{\infty,s}}\left(\sigma_r - \frac{\sigma_\varphi + \sigma_z}{2}\right), \ \varepsilon_{\varphi,s}^* = \frac{1}{E_{\infty,s}}\left(\sigma_\varphi - \frac{\sigma_r + \sigma_z}{2}\right),$$

$$\varepsilon_{z,s}^* = \frac{1}{E_{\infty,s}}\left(\sigma_z - \frac{\sigma_r + \sigma_\varphi}{2}\right), \ \varepsilon_{rz,s}^* = \frac{3}{2}\frac{\tau_{rz}}{E_{\infty,s}}.$$

In the absence of temperature effects, the total strains at $t \to \infty$ can be written as

$$\begin{aligned}
\varepsilon_r &= \frac{1}{E}(\sigma_r - \nu(\sigma_\varphi + \sigma_z)) + \left(\sigma_r - \frac{\sigma_\varphi + \sigma_z}{2}\right)\sum_{s=1}^{n}\frac{1}{E_{\infty s}}, \\
\varepsilon_\varphi &= \frac{1}{E}(\sigma_\varphi - \nu(\sigma_r + \sigma_z)) + \left(\sigma_\varphi - \frac{\sigma_r + \sigma_z}{2}\right)\sum_{s=1}^{n}\frac{1}{E_{\infty s}}, \\
\varepsilon_z &= \frac{1}{E}(\sigma_z - \nu(\sigma_r + \sigma_\varphi)) + \left(\sigma_z - \frac{\sigma_r + \sigma_\varphi}{2}\right)\sum_{s=1}^{n}\frac{1}{E_{\infty s}}, \\
\gamma_{rz} &= 2\varepsilon_{rz} = \frac{2(1+\nu)}{E}\tau_{rz} + 3\tau_{rz}\sum_{s=1}^{n}\frac{1}{E_{\infty s}}.
\end{aligned} \tag{19}$$

Equations (19) can be presented in the form

$$\begin{aligned}
\varepsilon_r &= \alpha^*\sigma_r - \beta^*\left(\sigma_\varphi + \sigma_z\right), \\
\varepsilon_\varphi &= \alpha^*\sigma_\varphi - \beta^*\left(\sigma_r + \sigma_z\right), \\
\varepsilon_z &= \alpha^*\sigma_z - \beta^*\left(\sigma_r + \sigma_\varphi\right),
\end{aligned} \tag{20}$$

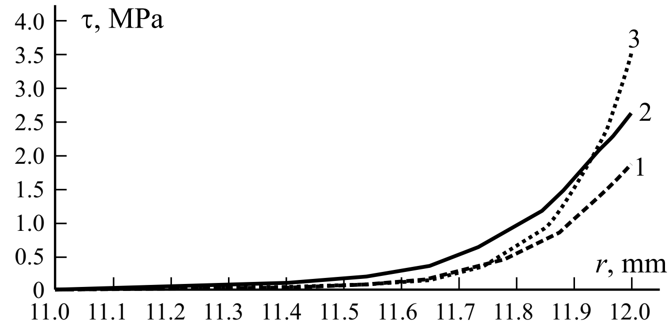

Fig. 7. The shear stress τ in the contact layer along the radius r at $t = 0$ (1), $t \to \infty$, $\gamma_{rz}^* \neq 0$ (2), and $t \to \infty$, $\gamma_{rz}^* = 0$ (3).

$$\gamma_{rz} = 2(\alpha^* + \beta^*)\tau_{rz},$$

where $\alpha^* = \frac{1}{E} + \sum_{s=1}^{n} \frac{1}{E_{\infty s}}$ and $\beta^* = \frac{\nu}{E} + \frac{1}{2}\sum_{s=1}^{n} \frac{1}{E_{\infty s}}$. Introducing the designations $\tilde{E} = 1/\alpha^*$ and $\tilde{\nu} = \beta^*/\alpha^*$, Eqs. (20) can be rewritten as

$$\varepsilon_r = \frac{\sigma_r - \tilde{\nu}\left(\sigma_\varphi + \sigma_z\right)}{\tilde{E}}, \quad \varepsilon_\varphi = \frac{\sigma_\varphi - \tilde{\nu}\left(\sigma_r + \sigma_z\right)}{\tilde{E}},$$
$$\varepsilon_z = \frac{\sigma_z - \tilde{\nu}\left(\sigma_r + \sigma_\varphi\right)}{\tilde{E}}, \quad \gamma_{rz} = \frac{2(1+\tilde{\nu})}{\tilde{E}}\tau_{rz}. \qquad (21)$$

Here, $\tilde{E}$ and $\tilde{\nu}$ are the long-term elastic modulus and long-term Poisson ratio. Thus, in order to obtain a solution at the end of creep, it is sufficient to replace the constants E and ν in the elastic solution by $\tilde{E}$ and $\tilde{\nu}$. Figure 7 shows shear stresses in the contact layer along the radius at $t = 0$ and $t \to \infty$ obtained by the indicated method using the FEM in combination with the contact-layer method. As in the previous graph, only the area in the immediate vicinity of the dangerous point is shown. At the end of the creep process, the maximum tangential stresses were 2.66 MPa, which practically coincides with the value indicated earlier for $t = 50{,}000$ h. Note that neglecting the shear creep strains in the contact layer leads to an overestimation of the tangential stresses at the end of creep. In this case, they were 3.57 MPa. The corresponding graph is also shown in Fig. 7. Thus, in general, creep strains increase the shear stresses, but their shear component partially reduces the stresses.

Conclusion

The presented calculation example shows the high efficiency of using the FEM in combination with the contact-layer method. In contrast to the solution obtained [9] using the finite-difference method, the FEM allows the mesh to be thickened at the point where the maximum stresses arise. On the basis of the approach proposed, it is found that neglecting the shear creep strains in the contact layer leads to an overestimation of the maximum shear stresses at the end of creep. The hypothesis of a linear distribution of shear stresses across the thickness of adhesive and substrate also overstates their values.

The reliability of the results of the work is confirmed by the results obtained by an analysis of the Maxwell–Gurevich equation at $t \to \infty$ and calculations using the long-term constants of the material found.

REFERENCES

1. N. Y. Tsybin, R. A. Turusov, and V. I. Andreev, “Comparison of creep in free polymer rod and creep in polymer layer of the layered composite,” Proc. Eng., **153**, 51-58 (2016).
2. V. I. Andreev, R. A. Turusov, and N. Y. Tsybin, “Application of the contact layer in the solution of the problem of bending the multilayer beam,” Proc. Eng., **153**, 59-65 (2016).
3. V. I. Andreev, R. A. Turusov, and N. Y. Tsybin, “Long strength of layered composite under normal fracture,” 5th Int. Conf. Advanced Design and Manufacturing Engineering, Atlantis Press, (2015).
4. R. A. Turusov, “Elastic and thermal behavior of a layered structure I. Experiment and theory,” Mech. Compos. Mater., **50**, No. 6, 801-808 (2015).
5. R. A. Turusov, “Elastic and thermal behavior of a layered structure. Part II. Calculation results and their analysis,” Mech. Compos. Mater., **51**, No. 1, 127-134 (2015).
6. V. Andreev, R. Turusov, and N. Tsybin, “The edge effects in layered beams,” IOP Conf. Ser: Materials Science and Engineering 21, Construction - The Formation of Living Environment, 042049 (2018).
7. V. I. Andreev, and R. A. Turusov, “Thermal strength of adhesion bond,” Appl. Mech. Mater., **670**, 153-157 (2014).
8. R. A. Turusov, and L. I. Manevich, “Contact-layer method in adhesive mechanics: Adhesive strength during normal detachment,” Polymer Sci. Ser. D., **3**, No. 3, 159-169 (2010).
9. A. S. Freidin, and R. A. Turusov, Properties and Calculation of Adhesive Joints, M., Publ. House Chem, (1990).
10. R. A. Turusov and L. I. Manevich, “Contact layer method: Determining parameters of rigidity and true strength of an adhesion bond for a contact layer,” Polymer Sci. Ser. D., **4**, No. 1, 1-4 (2011).
11. R. A. Turusov and L. I. Manevich, “The method of the contact layer in adhesion mechanics,” Glues Hermetics Technol., No. 6, 2-11 (2009).
12. R. A. Turusov, A. Y. Gorenberg, and B. M. Yazyev, “Long-term normal tearing strength of adhesive bonds,” Polymer Sci. Ser. D., **5**, No. 1, 7-14 (2012).
13. R. A. Turusov and L. I. Manevich, “Contact layer method in adhesive mechanics,” Polymer Sci. Ser. D., **3**, No. 1, 1-9 (2010).
14. R. A. Turusov and L. I. Manevich, “Introduction to adhesion mechanics,” Polymer Sci. Ser. D., **2**, No. 4, 209-213 (2009).
15. Turusov R. A., Kuperman A. M. Elastic properties of thin adhesive interlayers,” Polymer Sci. Ser. D., **7**, No. 1, 1-8 (2014).
16. K. Meguro and H. Tagel-Din, “Applied element method for structural analysis: Theory and application for linear materials,” Structural Eng./Earthquake Eng., Japan Soc. Civil Eng. (JSCE), **17**, 21-35 (2000).
17. A. S. Chepurnenko, A. A. Savchenko, and V. S. Chepurnenko, “Applied element method in the solution of plane problems in the theory of creep,” Mater. Phys. Mech., **42**, 455-460 (2019).
18. C. Grunwald, A. A. Khalil, B. Schaufelberger, E. M. Ricciardi, C. Pellecchia, E. De Iuliis, and W. Riedel, “Reliability of collapse simulation — Comparing finite and applied element method at different levels,” Eng. Struct., **176**, 265-278 (2018).
19. J. M. Adam, F. Parisi, J. Sagaseta, and X. Lu, “Research and practice on progressive collapse and robustness of building structures in the 21st century,” Eng. Struct., **173**, 122-149 (2018).
20. D. Malomo, R. Pinho, and A., “Penna Using the applied element method to simulate the dynamic response of full-scale URM houses tested to collapse or near-collapse conditions,” Earthquake Eng. Structural Dynamics., **47**, 1610-1630 (2018).
21. A. E, Dudnik, B. M. Yazyev, A. S. Chepurnenko, A. S. Denego, “Stress-strain state of a multilayer polymer pipe at nonlinear creep,” Izv. Kabardino-Balkar. Gos. Univ., No. 1, 37-41 (2016).
22. B. M. Yazyev et al., “The definition of a critical deflection of compressed rods with the creep by the method of Bubnov–Galerkin,” Materials Sci. Forum., **931**, 127-132 (2018).
23. B. M. Yazyev, S. V. Litvinov, and S. B. Yazyev, “Thermoviscoelasticity problem for a multilayer inhomogeneous polymeric cylinder,” Int. Polymer Sci. Technol., **36**, No. 2, 49-51 (2009).

24. A. S. Chepurnenko, “Stress-strain state of three-layered shallow shells under conditions of nonlinear creep,” Magazine Civil Eng., No. 8, 156-168 (2017).
25. A. L. Rabinovich, Introduction to the Mechanics of Reinforced Polymers [in Russian], Moscow, Nauka (1970).